Shock Waves (2000) 10: 229–234

Shock Waves

Oblique evaporation waves

J.R. Simões-Moreira

SISEA, Alternative Energy Systems Laboratory, Mechanical Engineering Department, Escola Politécnica da USP, Caixa postal 61548, São Paulo, SP, Brazil (e-mail: jrsimoes@usp.br)

Received 12 October 1999 / Accepted 21 March 2000

Abstract. Evaporation waves are processes that may occur under certain conditions in which a metastable or superheated liquid undergoes a sudden phase transition in a narrow and observable region, which resembles a shock wave. It is inferred from photographic documentation that in certain liquid jet flashing regimes the phenomenon is present. The evaporation wave discontinuity has been successfully modeled in a similar way as a deflagration wave in a combusting gas. One-dimensional laboratory experiments have demonstrated the existence of the (lower) Chapman-Jouguet solution for the cases where the liquid were at a high degree of metastability. Subsonic solutions were also observed for less pronounced degree of metastability (Hill 1991, Simões-Moreira 1994). In this paper, the fundamental theory is briefly revised and compared with some of the experimental results obtained for the cases operating at the C-J condition. Next, the paper presents the extension of the one-dimensional theory to include the oblique evaporation wave geometry. Relationships between upstream and downstream flow properties are discussed ant further consequences of these relationships are analyzed.

Key words: Evaporation wave, Metastable liquid, Evaporation, Phase transition, Liquid flashing

1 Introduction

Evaporation waves are abrupt adiabatic phase change processes that may occur in superheated or metastable liquids, as observed in some laboratory experiments (Grolmes and Fauske 1974; Thompson et al. 1987; Hill 1991; Simões-Moreira 1994; among others). The disturbance transforms superheated liquids into a high-speed two-phase flow at a lower pressure in a narrow and observable region, which resembles a shock wave discontinuity. An illustrative still picture of the phenomenon is shown in Fig. 1 taken from an evaporation wave progressing downward into a quiescent superheated liquid dodecane. The evaporation wave front slightly fluctuates perpendicularly to the tube axis as seen from high-speed moving pictures (Hill 1991; Simões-Moreira 1994), but the normal propagation mode is dominant and the evaporation front proceeds at a distinguishable and predictable average velocity. The length scale of the front of evaporation is relatively short, less than a tube diameter. Successful modeling of evaporation waves has been achieved by using an integral approach in which the laws of conservation are applied to a one-dimensional control volume enveloping the front of evaporation (Thompson et al. 1987; Hill 1991; Simões-Moreira 1994; Simões-Moreira and Shepherd 1999). Usual assumptions are that viscous and heat conduction effects are negligible outside the control volume. Also, thermal and mechanical equilibrium are valid simplifications for the two-phase flow downstream of the wave. Hill (1991) and Simões-Moreira (1994) provide a detailed discussion of the possible sustaining mechanisms of an evaporation wave front. The simple integral formulation drives the present analysis to the combustion field, specifically to the theory of deflagration waves in a combusting gas. Accordingly, the energy released in the combustion of a gas plays a similar role as the release of latent heat of vaporization in an evaporation wave. An important feature of this gas dynamic discontinuity is that there is a unique downstream solution known as the Chapman-Jouguet point for an upstream state and a given amount of heat released during the combustion process. Relevant properties of the C-J point are: 1– a maximum mass flow rate per unity of area across the deflagration wave is achieved, 2– the flow downstream is sonic in relation to the reacting combusting plane, and 3– the specific entropy jump is a local maximum. These flow dynamic characteristics are an indication of a choking condition. Experiments have shown that evaporation waves also have their C-J point (Thompson et al. 1987; Hill 1991; Simões-Moreira 1994). In addition, mass flow rates less than the maximum ones have also been obtained by the last two researchers depending on controlling the downstream pressure. Therefore, the evaporation wave phenomenon has both subsonic and sonic solutions as confirmed by laboratory experiments.

Much of the research efforts thus far have been concentrated on normal evaporation waves. Normal evaporation waves are those in which the front of propagation is perpendicular to the upstream and downstream velocities (Fig. 1). However, little or no attention has been given to modeling oblique evaporation waves, such as those ob-

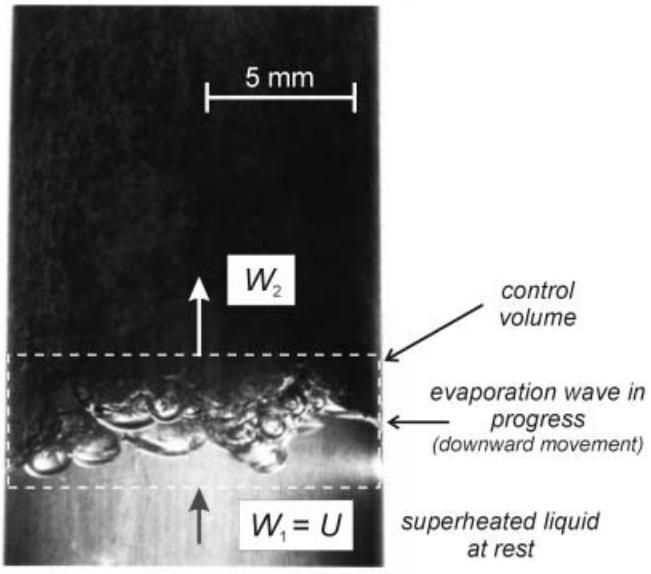

Fig. 1. An evaporation wave progressing in a quiescent superheated liquid dodecane (Simões-Moreira 1994). Measured data are $T_1 = 200°C$, $P_1 = 0.36$ bar, and $P_2 = 0.23$ bar. Estimated data are $U = 32.6$ cm/s and $x_2 = 36.8\%$ (run dd-p-110). The wave is moving downwards

served by Pasqua (1953), and Kim and O'Neal (1993) in the context of analyzing short orifice tubes as expansion devices. Also, short exposure time still pictures of experiments with flashing jets have shown a unique feature in which there is a visible discontinuity front where the phase transition occurs (Reitz 1990; Kurschat et al. 1992; Athans 1995; among others) at the exit section or somewhere more downstream as the liquid exits the nozzle. It is inferred from the photographic documentation that the superheated liquid refrigerant inside the short tube or the flashing liquid expanding in a nozzle undergoes a continual phase transition process forming a slanted interfacial region until the superheated liquid is evaporated resulting in a high-speed two-phase mixture. This slanted interfacial region is modeled in the present work as an oblique evaporation wave.

This paper has the goal of presenting the relevant properties of a normal evaporation wave firstly. Next, the theory of normal evaporation waves is expanded to include the oblique geometry commonly present in some flashing jets. The theory is particularly devoted to obtaining the relationship between the wave angle and the turning angle of such flows as well as discussing the main properties and how they are related to the experimental results. Usefulness of evaporation waves studies include analyzing accidents such as sudden rupture of vessels that may occur in power generation and chemical industries, and liquefied-gas pipelines as well. Also, the phenomenon may be present in expansion devices of refrigeration cycles and in fluid injectors. In principle, the phenomenon can occur in any system where sudden expansion of a superheated liquid may be present.

2 Normal evaporation waves

Consider a control volume capturing the steady evaporation wave and moving with it (Fig. 1). The laws of conservation of mass, momentum, and energy can be written respectively as

$$[J] = \left[\frac{W}{v}\right] = 0, \tag{1}$$

$$[P + WJ] = 0, \text{ and} \tag{2}$$

$$\left[h + \frac{W^2}{2}\right] = 0, \tag{3}$$

where the square brackets indicate a jump in the enclosed value, i.e., $[f] = f_2 - f_1$, v is the specific volume, W is the relative fluid velocity, P is the pressure, h is the specific enthalpy, and J is the superficial mass flux, i.e., the mass flow rate per unit of area. Subscripts "$_1$" and "$_2$" are for upstream (superheated liquid) and downstream (two-phase mixture) states, respectively. By combining Eqs. (1) and (2), one obtains the Rayleigh equation

$$J^2 = -\frac{[P]}{[v]}. \tag{4}$$

Classical analysis of the Rayleigh equation reveals that the downstream solution lies on a straight line on the $P-v$ diagram. It is known that the superficial mass flow rate will first increase as the downstream pressure decreases. This will continue to hold true down to the pressure corresponding to the C-J one. For downstream pressures lower than the C-J pressure, that functional trend will be reversed. Therefore, the C-J point is a condition of maximum superficial mass flow rate. The mathematical statement of maximum superficial mass flow rate is given by $dJ^2 = 0$. Also, it can be proved that at the C-J point the specific entropy jump is also a local maximum as well as a sonic point as informed in the introductory section. It is straightforward to show that, for a given upstream state 1, the condition of maximum applied to Eq. (4), i.e., the C-J point, results in

$$\frac{dv_2}{dT_2} = -\frac{1}{J^2_{\mathrm{C-J}}}\frac{dP_2}{dT_2}. \tag{5}$$

The downstream specific volume is given by the simple mixture rule $v_2 = (1 - x_2)v_{L2} + x_2 v_{V2}$. The subscripts "$_L$" and "$_V$" are for liquid and vapor phases, and the subscript "$_{\mathrm{C-J}}$" was added in order to indicate the solution uniqueness. Implicitly assumed is the hypothesis that the downstream two-phase mixture is homogeneous and is in thermal and mechanical equilibrium. Combining the three conservation equations (1–3), one can obtain the downstream vapor quality, x_2, resulting in

$$x_2 = \frac{2\,(h_1 - h_{\mathrm{L2}}) + (v_{\mathrm{L2}} + v_1)\,[P]}{2\,(h_{\mathrm{V2}} - h_{\mathrm{L2}}) - (v_{\mathrm{V2}} - v_{\mathrm{L2}})\,[P]}. \tag{6}$$

By substituting J from the Rayleigh equation (4) into Eq. (5), Eqs. (5) and (6) can be solved numerically, along

with an equation of state (or a thermodynamic table) valid for the saturation region to obtain the C-J point for a given upstream state. Note that all downstream properties depend only on T_2, given the upstream state 1 of the superheated liquid. A Newton-Raphson solution scheme has been used for the examples presented in this paper (Table 1). Numerical differentiation was used whenever necessary. As a result of the solution of these two equations, the downstream vapor quality, x_2, and the temperature, T_2, are obtained.

Table 1 illustrates some experimental results and the corresponding numerical solutions for some data obtained by the author in 1-D experiments with the superheated liquid at rest ($U = W_1$). Initial data refer to superheated liquid properties, which are the temperature T_1, saturation pressure P_σ, pressure P_1, and specific volume v_1. Measured data are the downstream pressure P_2 and wave velocity U. The last three columns, labeled "calculated properties", refer to the calculated properties at the C-J point for the initial average data, which are: P_2, U, x_2, and v_2. The calculated C-J points are reasonably well predicted. The deviations are due to the nature of the homogeneous two-phase flow model, which has been found to usually underestimate the downstream pressure and wave velocity (Simões-Moreira 1994). A more realistic approach requires the use of more elaborated two-phase models, considering, for instance, slip between phase velocities as analyzed by the author (also see Simões-Moreira and Shepherd 1999). Furthermore, as accomplished in previous studies, the present procedure avoids the use of any correlation for the speed-of-sound of the two-phase medium downstream of the wave. Therefore, the principle of maximum mass flow rate alone suffices to close the problem. Implicitly assumed in the present formulation is that the downstream state is a two-phase mixture. However, for a class of fluids known as retrograde, there exists the possibility of a complete phase change process in a evaporation wave (Simões-Moreira et al. 1993).

3 Oblique evaporation waves

Oblique evaporation waves may occur in flashing jets, and inside short orifices, and valves passages under certain conditions. Differently from a normal evaporation wave, in an oblique evaporation wave the main relative superheated liquid velocity is inclined to the evaporating front, as illustrated by the velocity diagram in Fig. 2. As before, the reference frame moves attached to the wave front, so that the wave seems to be stationary. In a laboratory frame the wave moves at a velocity $\mathbf{U}$ and the superheated liquid moves at a velocity $\mathbf{u}_1$. A tangential plane to the evaporation front and the upstream relative velocitiy $\mathbf{u}_1 - \mathbf{U}$ forms an angle β, which is called the "wave angle". The relative tangential velocity component is $\mathbf{t}$ and the relative normal velocity components are $\mathbf{W}_1$and $\mathbf{W}_2$. The main fluid velocity turns an angle θ as the fluid crosses the wave. θ is the "turning angle". Oblique evaporation waves have many similar properties to a regular oblique compression shock wave (see Thompson 1988, for instance), which are:

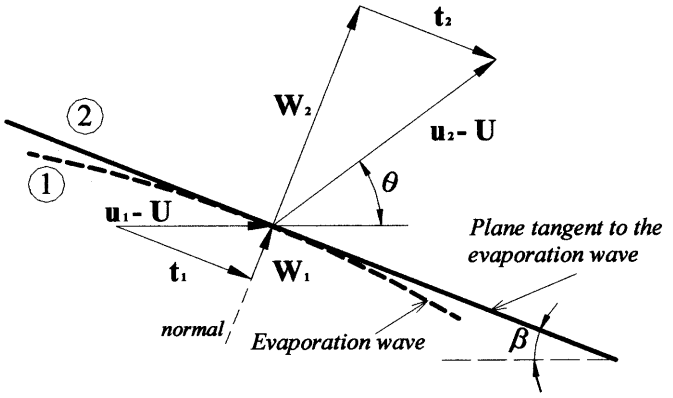

Fig. 2. Geometry of an oblique evaporation wave

1 – the relative velocities, $\mathbf{u}_1 - \mathbf{U}$ and $\mathbf{u}_2 - \mathbf{U}$, are coplanar with the vectors normal to the wave front. This means that the fluid velocity bends as it traverses the evaporation wave front but stays in the same plane. 2 – the tangential velocity component is invariant across the wave, i.e., $\mathbf{t} = \mathbf{t}_1 = \mathbf{t}_2$. Further implication of this property is that one can transform an oblique evaporation wave into a normal evaporation wave by adding the tangential component to the wave velocity. 3 – the stagnation specific enthalpy h_0 is invariant in a stationary oblique evaporation wave ($\mathbf{U} = 0$), i.e., $h_0 = h_1 + u_1^2/2 = h_2 + u_2^2/2$. On the side of dissimilar properties, the normal component velocity jump $[W]$ is always positive for an evaporation wave. The reason for this is that an increase in the downstream specific volume due to evaporation must be accompanied by a correspondent increase of W_2, as mass flux must be conserved (Eq. (1)). Therefore, evaporation waves accelerate the flow, i.e., $W_2 > W_1$, since $v_2 > v_1$, contrary to the normal component of a regular oblique shock wave. Also, in opposition to an oblique shock wave, the fluid turns away from the evaporation front. Referring to Fig. 2, the following relationship between θ and β exists

$$\tan\theta = \frac{\sin 2\beta}{2\left(\sin^2\beta + \dfrac{W_1}{[W]}\right)}. \tag{7}$$

If the mass conservation equation (1) is used, a further simplified form of Eq. (7) is still possible

$$\tan\theta = \frac{\sin 2\beta}{2\left(\sin^2\beta + \dfrac{1}{(v_2/v_1) - 1}\right)}. \tag{8}$$

In the wave angle range between 0° and 90° and knowing that the two-phase specific volume is necessarily higher than the superheated liquid specific volume, that is, $(v_2/v_1) > 1$, the turning angle θ has the same sign as the wave angle β, which corroborates the shock geometry depicted in Fig. 2. The problem is totally symmetric for $90° < \beta < 180°$. In any situation the fluid bends away from the evaporation front. It is noteworthy to say that a high specific volume ratio across an evaporation wave is expected, typically in the order of 20. The graphics of Fig. 3 presents the dependence of the turning angle with

Table 1. Experimental data and numerical C-J results for superheated dodecane

initial data				measured data		calculated properties[4]				
$T_1^{(1)}$ (°)	$P_1^{(2)}$ (bar)	$P_\sigma^{(3)}$ (bar)	$v_1^{(3)}$ (m^3/kg)	$P_2^{(2)}$ (bar)	$U^{(2)}$ (cm/s)	T_2 (°)	P_2 (bar)	U (cm/s)	x_2 (%)	v_2 (m^3/kg)
180	0.24 ± 0.02	0.392	0.00156	0.18 ± 0.01	25.3 ± 0.6	152	0.16	24.8	26.7	0.3386
200	0.33 ± 0.02	0.676	0.00160	0.22 ± 0.01	30.9 ± 0.6	158	0.20	28.8	40.1	0.4134
216	0.44 ± 0.01	1.005	0.00164	0.28 ± 0.02	39.0 ± 0.7	166	0.26	36.0	49.0	0.3935
230	0.59 ± 0.02	1.387	0.00167	0.37 ± 0.01	47.2 ± 0.8	176	0.35	46.2	55.1	0.3339
250	0.83 ± 0.04	2.118	0.00172	0.52 ± 0.03	64.8 ± 0.8	187	0.48	60.6	67.1	0.3013
270	1.19 ± 0.02	3.118	0.00178	0.73 ± 0.01	83.7 ± 1	200	0.68	83.4	78.2	0.2519
290	1.91 ± 0.04	4.449	0.00185	1.16 ± 0.01	138 ± 3	220	1.10	132.8	84.9	0.1721
300	2.12 ± 0.07	5.260	0.00190	1.32 ± 0.07	158 ± 6	224	1.21	143.3	93.9	0.1735

(1) accuracy: ±1°C; (2) accuracy: $\pm 2\sigma$; (3) properties calculated using the Lee and Keslers's equation of state and other correlations (see Simões-Moreira 1994 for details); (4) C-J points obtained from average values.

the wave angle parameterized by several ratios of specific volumes, v_2/v_1. The turning angle is upper bounded by the straight line $\theta = 90° - \beta$ as the wave angle increases. This result can also be easily obtained from Eq. (8) by neglecting the contribution of the second term between brackets in the denominator. On the other hand, if the wave angle is reduced, the turning angle θ undergoes initially an almost linear increase followed by a sharp decrease, giving rise to points of maximum turn (details in minor graph of Fig. 3). These extreme conditions can be obtained by differentiating Eq. (8) with respect to β and setting it to zero, as usual. In doing so, one will obtain, after some manipulation, the simple expression

$$\tan\theta_{\max} = \frac{(v_2/v_1) - 1}{2\sqrt{v_2/v_1}}. \tag{9}$$

The corresponding wave angle $\beta_{\max}$ where the maximum fluid turning occurs is given by

$$\sin\beta_{\max} = \frac{1}{\sqrt{(v_2/v_1) + 1}}. \tag{10}$$

By combining Eqs. (9) and (10), one can obtain a relationship between $\beta_{\max}$ and $\theta_{\max}$,

$$\theta_{\max} = 90^{\circ} - 2\beta_{\max}. \tag{11}$$

The above expression corresponds to the dashed line seen in Fig. 3. The present analytical findings are very similar to the ones for oblique flame fronts (Emmons 1958) as far as the point of view of fluid dynamics is concerned. The main difference is related to the range of specific volume ratios. High specific volume ratios are expected (order of 20) in the former case, while in the latter case considerable lower ratio values are usually observed.

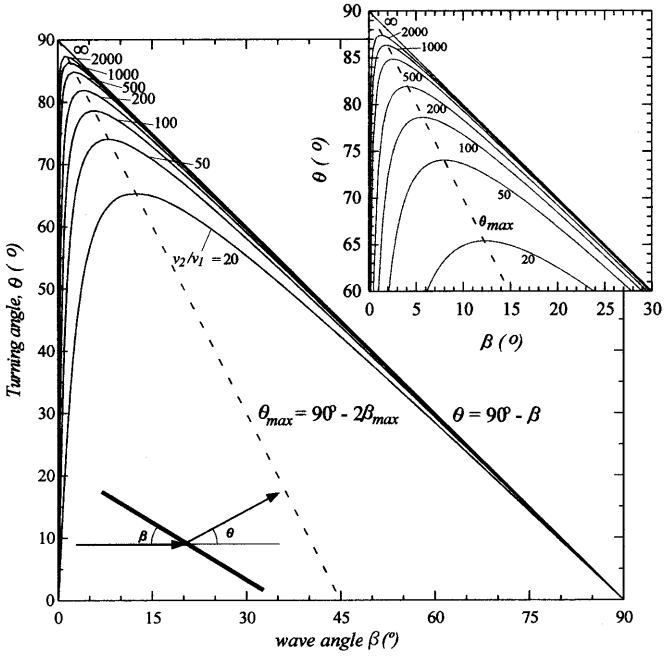

Fig. 3. Turning angle θ as a function of the evaporation wave angle β for several specific volume ratios. Minor graphics shows details around maximum turning angles

4 General comments on evaporation waves geometry

Moving pictures (see also Fig. 1) obtained by Hill (1991) and this author (1994) have shown that as the evaporation wave front proceeds into the quiescent superheated liquid, the wave sways around an average plane normal to the axis of the containing tube. Nevertheless, the wave follows, in average, the 1-D geometry of the tube. Thus, it is fair to ask if the one-dimensional constraint dominates and the flow is "straightened" whenever β deviates from 90°. What are the stabilizing effects that drive and sustain a normal evaporation wave in such conditions are still to be understood.

A different wave front geometry has been observed when the superheated liquid is set into motion, such as in the experiments with short tubes (Pasqua 1953; Kim and O'Neal 1993) and flashing jets (Reitz 1990; Kurshat

et al. 1992; Athans 1995; among others). From the photographic documentation, one can conclude that there exists a front of evaporation, which is oblique to the main superheated liquid velocity. As a consequence, the present theory should apply. Figure 4a is one of the several still pictures obtained by Athans in experiments with flashing iso-octane discharging into a large low-pressure reservoir. Figure 4b is the corresponding schematic drawing. Using suitable illumination techniques, Athans was able to see that as the superheated liquid iso-octane exited a small converging nozzle (id = 0.864 mm), a main liquid core was still visible several diameters downstream (gleaming central area in figure) while the liquid was undergoing a phase transition at the surface of that core. As the evaporation process occurred, the fluid bent away from the core as illustrated in the figure. Since the jet expands freely without any geometrical constraint, it is expected that the fluid would follow closely, but not necessarily, the line of maximum turning angles (dashed line in Fig. 3), which means that β is low and θ is close to 90°. This seems to be the case, at least for the jet in the vicinity of the exiting section as seen in Fig. 4a and illustrated in Fig. 4b. On the other hand, it is not possible to completely close the problem of the flashing jet at this point, as a degree of indeterminacy exists associated with the thermodynamic state of the liquid jet, particularly the exiting section pressure. Once the pressure magnitude is determined, mass flow rate is promptly obtained for a known isentropic nozzle as well as other flow parameters, such as the exiting liquid velocity. Alternatively, exiting liquid velocity will furnish the unknown pressure. Given the thermodynamic state of exiting superheated liquid state, the turning and wave angles of the oblique evaporation wave can be calculated as well as the liquid jet extinction length for a constant evaporation rate hypothesis. Unfortunately, to the knowledge of this author no one so far has been able to measure either the exiting liquid pressure or velocity for the obvious reason of experimental difficulties. Likewise, no progress has been made in the theoretical field.

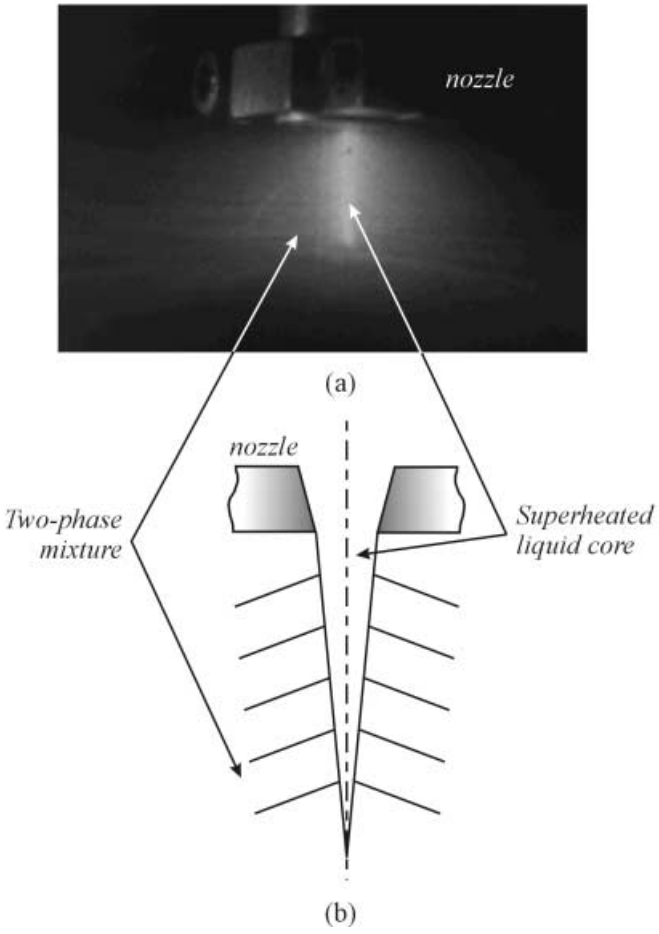

Fig. 4. a Still picture of flashing jet iso-octane issuing from a converging nozzle (expt 9 - obtained from Athans 1994). Main core is superheated liquid. Initial temperature = 223 °C; injection pressure = 2068 kPa, pressure chamber = 0.52 kPa; nozzle exit diameter = 0.864 mm; **b** schematics diagram showing the oblique front

5 Conclusions

Evaporation waves are adiabatic, rapid phase transition phenomenon, which are characterized by a jump in flow properties in a narrow and observable interface. Successful modeling has been achieved by treating the discontinuity in a similar fashion as a deflagration wave. This study presented a brief review of the integral formulation of normal evaporation waves, emphasizing a procedure to calculate the Chapman-Jouguet point for a given upstream superheated liquid state. The calculated C-J points agree well with the experimental results. In the second part of this paper, the case of oblique evaporation waves and the relationship between the wave angle and the turning angle were analyzed. It was found that the theory of oblique evaporation waves is very similar to the one for oblique deflagration waves (oblique flame). Qualitative experimental observations from literature corroborate the present analysis.

Acknowledgements. The author would like to acknowledge the personal discussion with Dr. R. Athans on some photographic techniques used in his Ph. D. thesis. This work was supported by FAPESP - Fundação de Apoio à Pesquisa do Estado de São Paulo, Brazil.

References

Athans RE (1995) The rapid expansion of near-critical retrograde fluid. Ph.D. Thesis, Rensselaer Polytechnic Institute, Troy, NY

Emmons H (1958) Gas dynamics of combustion and detonation, In: Emmons H (ed) Fundamentals of Gas Dynamics, III, Princeton Univ. Press

Grolmes MA and Fauske HK (1974) Axial propagation of free surface boiling into superheated liquids in vertical tubes. Proceedings of 5th International Heat Transfer Conference, Tokyo, Japan, 4, pp 30–34

Hill L (1991) An experimental study of evaporation waves in a superheated liquid. Ph.D. Thesis, California Institute of Technology, Pasadena, CA

Kim Y and O'Neal DL (1993) An experimental study of two-phase flow of HFC-134a through short tube orifices. Heat Pump and Refrigeration Systems Design, Analysis, and Applications, AES-ASME 29, pp 1–8

Kurschat Th, Chaves H, and Meier GEA (1992) Complete adiabatic evaporation of highly superheated liquid jets. Journal of Fluid Mechanics 236, pp 43–59

Pasqua, PF (1953) Metastable flow of freon-12. Refrigerating Engineering 61, pp 1084–1089

Reitz RD (1990) A photographic study of flash-boiling atomization. Aerosol Science and Technology 12, pp 561–569

Simões-Moreira JR (1994) Adiabatic evaporation waves. Ph.D. Thesis, Rensselaer Polytechnic Institute, Troy, NY

Simões-Moreira JR and Shepherd J (1999) Evaporation waves in superheated dodecane. Journal of Fluid Mechanics 382, pp 63–86

Simões-Moreira JR, McCahan SM, and Shepherd J (1993) Complete evaporation waves. ASME Fluid Engineering Conference, paper 93-FE-7, ASME, Washington, DC

Thompson, PA, Chaves H, Meier G, Kim YG, and Speckman HD (1987) Wave splitting in a fluid of large heat capacity. Journal of Fluid Mechanics 185, pp 43–59

Thompson, PA (1988) Compressible-Fluid Dynamics. 1st edn., McGraw-Hill, New York